Carbohydrate Polymers 92 (2013) 321–327

Contents lists available at SciVerse ScienceDirect

Carbohydrate Polymers

journal homepage: www.elsevier.com/locate/carbpol

A comparison of spacer on water-soluble cyclodextrin grafted chitosan inclusion complex as carrier of eugenol to mucosae

Warayuth Sajomsang[a], Onanong Nuchuchua[a], Somsak Saesoo[a], Pattarapond Gonil[a], Saowaluk Chaleawlert-umpon[a], Nuttaporn Pimpha[a], Issara Sramala[a], Apinan Soottitantawat[b], Satit Puttipipatkhachorn[c], Uracha Rungsardthong Ruktanonchai[a,*]

[a] National Nanotechnology Center, National Science and Technology Development Agency, Thailand Science Park, Pathumthani, Thailand
[b] Department of Chemical Engineering, Faculty of Engineering, Chulalongkorn University, Bangkok, Thailand
[c] Department of Manufacturing Pharmacy, Faculty of Pharmacy, Mahidol University, Bangkok, Thailand

ARTICLE INFO

Article history:
Received 2 July 2012
Received in revised form 24 August 2012
Accepted 27 August 2012
Available online 1 September 2012

Keywords:
Chitosan
Cyclodextrin
Eugenol
Mucoadhesive
Buccal
Mucosal carrier

ABSTRACT

In this study two types of water-soluble βCD grafted chitosan were synthesized and compared based on similar degree of N-substitution of βCD moiety; QCD23-*g*-CS contained methylene spacer and QCDCA22-*g*-CS contained citric acid spacer. The QCD23-*g*-CS demonstrated greater eugenol (EG) encapsulation efficiency than that of QCDCA22-*g*-CS. The micelle-like assemblies of QCD23-*g*-CS led to slower release of EG while it did not observe in case of QCDCA22-*g*-CS. It was found that EG could absorb on chitosan backbone according to in silico modeling. Cytotoxicity of both derivatives against buccal mucosa cell is concentration-dependent. The QCDCA22-*g*-CS demonstrated stronger mucoadhesive response than that of QCD23-*g*-CS, due to hydrogen bonding according to mucin particle and SPR methods. Our results revealed that the spacer on both derivatives played an important role on binding affinity with EG, releasing profile and mucoadhesive property. These derivatives could be considered as promising carriers for mucosal delivery system.

1. Introduction

It is well known that cyclodextrins (CDs) or cyclomaltoheptaoses are a series of cyclic oligosaccharides which composed of 6–8 D-glucose units and named as α-, β-, and γ-CD, respectively (Szejtli, 2004). The CDs have hydrophobic cavity, which is convenient for assembling various lipophilic molecules from hydrophobic interactions (Nuchuchua et al., 2009; Zhan, Jiang, Wang, Li, & Dong, 2008). The CDs are widely used as enabling excipients in numerous marketed drug formulations (Shimpi, Chauhan, & Shimpi, 2005; Song, Bai, Xu, He, & Pan, 2009), however, limited application of the CDs is the absence of mucoadhesive property. In order to improve mucoadhesive property of the CDs, the CDs must be introduced into the bioadhesive polymer backbone. In this study, isolated chitosan (CS) is the linear and partly acetylated (1-4)-2-amino-2-deoxy-β-D-glucan (Muzzarelli, 1977; Ravi Kumar, Muzzarelli, Muzzarelli, Sashiwa, & Domb, 2004), was used as a bioadhesive polymer since it has non-toxic, biodegradable, and the most pertinent biocompatible properties (Illum, Farraj, & Davis, 1994; Muzzarelli, 2010). Moreover it has shown to be one of mucoadhesive cationic polymers at acidic pH values (Sajomsang, Ruktanonchai, Gonil, & Nuchuchua, 2009; Takeuchi et al., 2005). In order to combine the advantages of both CD and chitosan, the CD grafted chitosan has recently gained interest because it can be widely used in various fields (Prabaharan & Gong, 2008; Prabaharan & Jayakumar, 2009; Prabaharan & Mano, 2006; Van De Manakker, Vermonden, Van Nostrum, & Hennink, 2009). Therefore, introduction of CD moieties into the chitosan backbones may lead to a molecular carrier that possess the cumulative effects of inclusion, size specificity and transport properties of CDs as well as the controlled release ability of the polymeric matrix. However, major applications of the CD grafted chitosan remain limited due to their low water-solubility. In order to improve water solubility of the CD grafted chitosan, two types of water-soluble βCD grafted chitosan were developed by our research group (Chaleawlert-umpon et al., 2011; Gonil et al., 2011). The synthetic routes were carried out by two steps. The βCD grafted chitosan with different spacers were synthesized in the first step. The last step, quaternization by using glycidyltrimethyl ammonium chloride (GTMAC) as a quaternizing agent was used to make permanent cationic charges into the βCD grafted chitosan backbone. The quaternized βCD grafted chitosan with methylene spacer was abbreviated QCD-*g*-CS while quaternized βCD grafted

* Corresponding author. Tel.: +66 02564 7100x6552; fax: +66 02564 6981.
E-mail address: uracha@nanotec.or.th (U.R. Ruktanonchai).

0144-8617/$ – see front matter © 2012 Elsevier Ltd. All rights reserved.
http://dx.doi.org/10.1016/j.carbpol.2012.08.106

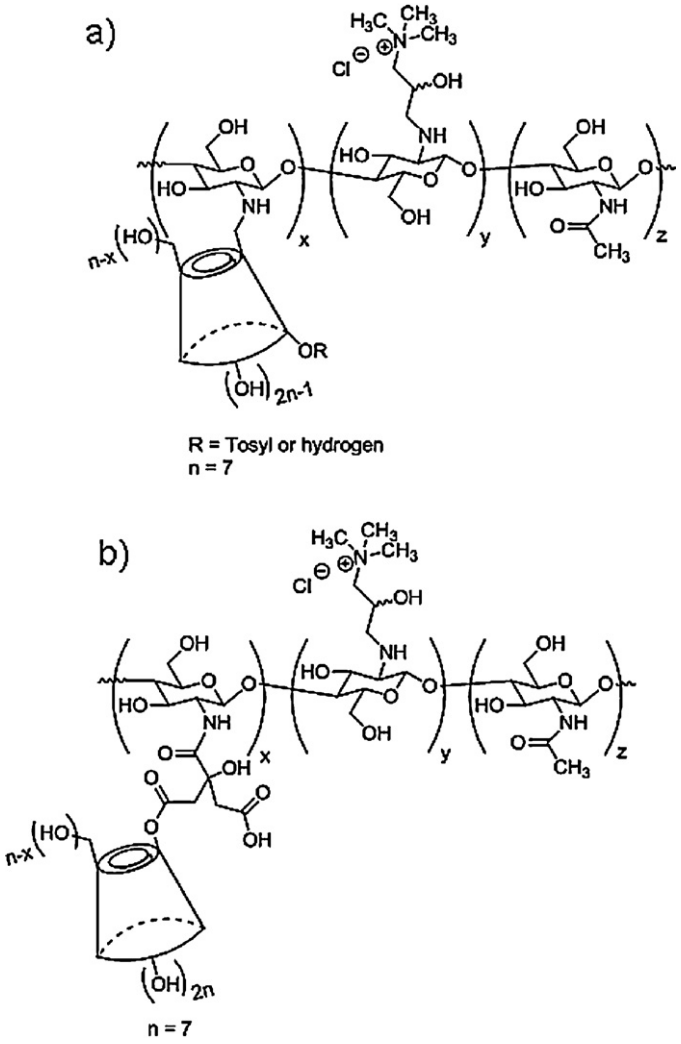

Fig. 1. Chemical structures of QCD23-*g*-CS (a) and QCDCA22-*g*-CS (b).

chitosan with citric acid spacer was abbreviated QCDCA-*g*-CS. The chemical structures of both quaternized βCD grafted chitosan with different spacers are shown in Fig. 1. In this work, we aimed to investigate the role of chemical structure of QCD23-*g*-CS and QCDCA22-*g*-CS at fixed degree of N-substitution (DS) of βCD to 22–23% on EG encapsulation efficiency and release profile. Moreover, mucoadhesive property of these derivatives was investigated by comparing on two methods, which are sub-micron mucin particle method and surface plasmon resonance (SPR).

2. Materials and methods

2.1. Materials

The following materials were of analytical grade from indicated sources without further purification. Chitosan (CS) with an average molecular weight (M_w) of 22 kDa was from Seafresh Chitosan Lab (Bangkok, Thailand). The degree of deacetylation (DDA) of chitosan was 90% by ^{1}H NMR spectroscopy. Mucin (type III) from porcine and eugenol (EG) were from Sigma–Aldrich Co. (Virgin Islands, USA). β-Cyclodextrin (βCD) was from Wacker Chemical AG (Munich, Germany). Sabourand's dextrose agar (SDA), Sabourand's dextrose broth (SDB), brain heart infusion agar (BHA), brain heart infusion broth (BHB) were from Becton (New Jersey, USA). Methanol, Na_2HPO_4, KH_2PO_4 and sodium chloride were from Fisher Scientific (Loughborough, UK). MTT (3-(4,5-dimethyldiazol-2-yl)-2,5 diphenyl Tetrazolium Bromide, Dulbecco's modified Eagle's medium (DMEM) and F12 were from GIBCO Invitrogen (Grand Island, NY, USA). Fetal bovine serum (FBS) was from Biochrom AG (Berlin, Germany). L-Glutamine, penicillin G sodium, streptomicin sulfate, and amphotericin B were from Invitrogen Corp. (Carlsbad, CA, USA). Dimethylsulfoxide (DMSO) was from Sigma–Aldrich, Inc. (Poole, Dorset, UK). The deionized (DI) water was produced from a MilliQ Plus (Millipore, Schwalbach, Germany). The microorganisms used in the inhibitory test were from the Department of Medical Sciences (Ministry of Public Health, Thailand). Microorganisms used in the study were *Candida albicans* ATCC 10231, *Streptococcus oralis* ATCC 35037T and *Streptococcus mutant* ATCC 25175T. Buccal mucosa cell was JCRB 0831 (HO-1-N-1) was from Japanese Collection of Research Bioresources (JCRB), Japan.

2.2. Synthesis of β-cyclodextrin grafted chitosan with different spacers (CD-g-CS and CDCA22-g-CS)

The CD23-*g*-CS was carried out by reacting chitosan with O-*p*-toluenesulfonyl-β-cyclodextrin (Ts-CD) under acidic condition and high temperature in the presence of DMF (Gonil et al., 2011) while the CDCA22-*g*-CS was prepared by amide formation between amine groups of chitosan and free carboxyl groups of β-cyclodextrin citrate under acidic condition and high temperature (Chaleawlert-umpon et al., 2011) which previously reported by our research group. The DS of βCD was fixed about 22–23% grafting, and it was abbreviated CD23-*g*-CS and CDCA22-*g*-CS for methylene spacer and citric acid spacer, respectively.

2.3. Synthesis of quaternized β-cyclodextrin grafted chitosan (QCD23-g-CS and QCDCA22-g-CS)

Quaternization of the CD23-*g*-CS and CDCA22-*g*-CS was carried out by using GTMAC as a quaternizing agent under acidic condition and high temperature which previously reported by our research group. Finally, water-soluble CD23-*g*-CS and CDCA22-*g*-CS were obtained, and it was abbreviated QCD23-*g*-CS and QCDCA22-*g*-CS for methylene spacer and citric acid spacer, respectively.

2.4. Preparation of inclusion complex

The QCD23-*g*-CS and QCDCA22-*g*-CS were completely dissolved in deionized water at concentration of 1% w/v. EG was then added at 1:1 mole ratio between βCD and EG. The solution was shaken at 25 °C, 250 rpm for 4 h, and lyophilized by Gamma 2-16 LSC (Christ, UK). The dried powder was then kept in gas-tight bottles at 4 °C until further analysis.

2.5. Determination of % encapsulation efficiency (%EE)

An amount of EG in inclusion complex was determined by methanol extraction method. In brief, 12 mL of methanol was mixed with 50 mg of the complex. The mixtures were vigorously shaken at 60 °C, 250 rpm for 8 h. The supernatants were separated by centrifugation (MR231, Thermo Scientific, USA) under 7500 rpm, 30 °C for 30 min, and then measured by UV spectrophotometer (Labmolecular dynamica 650, Perkin Elmer, USA) at the wavelength of 281 nm. %EE can be calculated as followed:

$$\%EE = \frac{\text{Extracted EG (mg) in methanol} \times 100}{\text{Initial loaded EG (mg)}} \quad (1)$$

2.6. Computer modeling of inclusion complex between QCD23-g-CS and QCDCA22-g-CS with EG

2.6.1. Thermodynamic properties of the inclusion complex in vacuum

The molecular dynamic simulations were performed using Material Studio version 4.3 (Accelrys, Boston, USA). A COMPASS force field was used throughout the study. The structures of βCD, QCD23-*g*-CS and QCDCA22-*g*-CS with EG were constructed and subjected to geometry optimization. The optimized structures of EG were then subjected to an absorption locator module with various derivatives as absorption substrates. The models were constructed at fixed mole ratio of EG to βCD in both QCD23-*g*-CS and QCDCA22-*g*-CS at 1:1. Free energy of complex formation ($E_{complex}$) and the binding energy for the models, a summation of intra-molecular distortion ($E_{distortion}$) and inter-molecular interaction ($E_{non\text{-}bond}$) energy terms were expressed as:

$$E_{complex} = E_{distortion} + E_{non\text{-}bond} = (E_b + E_\theta + E_\phi) + (E_{vdW} + E_{Coulomb}) \quad (5)$$

where E_b is the bond stretching energy, E_θ is the valence angle bending energy, E_ϕ is the dihedral torsion energy, E_{vdW} is the Van der Waals interaction energy, and $E_{Coulomb}$ is the coulombic interaction energy.

2.6.2. Thermodynamic properties in water system

Models of QCD23-*g*-CS and QCDCA22-*g*-CS and their inclusion complex with EG were constructed as described above. The amorphous structures of the host–guest inclusion complex were generated under periodic boundary conditions. The lengths of the cell were over 20.0 Å × 20.0 Å for the inclusion complex with the addition of 500 molecules of water to adjust in the system. The densities of βCD and EG in the systems were maintained in synthia units at 1.27 and 0.87 g/cm^3 at 298 K, respectively. Of ten configurations, only one system was chosen according to its lowest energy as given by molecular mechanics calculations as the initial configuration. To remove unfavorable interactions in the initial configuration, 5000 steps of energy minimization were employed using Smart algorithm.

Molecular dynamic simulation for 100 ps was carried out using normal pressure and temperature conditions with a time step of 1 fs in a range of 273–310 K. A cut-off distance of 9.0 Å and a buffer of 0.5 Å were adopted to minimize calculation of the non-bond interactions. Electrostatic charges of the model were calculated by the charge equilibration method. The duration of the equilibration dynamics was equal to 100 ps. Models of inclusion complex were then subjected to molecular dynamics for at least 1000 ps. Each of equilibrated EG: βCD in both QCD23-*g*-CS and QCDCA22-*g*-CS water systems were then subjected to free energy calculation. The total free energy (ΔG) of each complex model in water-explicit system was calculated by the procedure proposed by Fermeglia's group (Fermeglia, Ferrone, Lodi, & Prici, 2003) as briefly described below. According to this method, ΔG_{bind} is calculated as follows:

$$\Delta G = \Delta G_{bind} + \Delta G^{C}_{sol} - \Delta G^{EG}_{sol} - \Delta G^{CD}_{sol} \quad (6)$$

where ΔG_{bind} is the complex formation energy ($E_{complex}$) between EG and βCD, ΔG^{C}_{sol}, ΔG^{EG}_{sol} and ΔG^{CD}_{sol} are the solvation free energy for the inclusion complex, EG and βCD, respectively.

All energetic analysis was performed only for a single molecular dynamic trajectory of the inclusion complex considered, with unbound βCD in QCD23-*g*-CS and QCDCA22-*g*-CS and EG snapshots taken from the snapshots of that trajectory. The hydrogen calculation was performed by hydrogen build following this geometric parameter: the hydrogen-acceptor distance <3.0 Å and the donor-hydrogen–acceptor angle > 90.0°.

2.7. In vitro release study

Five milligrams of solid inclusion complex at 1:1 mole ratio were contained in dialysis tube with Spectra/Por® MWCO 100–500 Da (Spectrum Laboratories Inc., Rancho Dominguez, Canada) and immersed in 10 mL of 30:70 (v/v) methanol and simulated saliva buffer (16 mM Na_2HPO_4, 1.2 mM KH_2PO_4 and 0.14 M NaCl at pH 6.8). The tubes were placed at 32.0 ± 0.5 °C in shaking incubator (Vision Scientific Co., Ltd., Kyunggi-do, Korea) with shaking speed of 100 rpm. At each time point, 1 mL of buffer was collected and EG contents were analyzed by UV spectrophotometer as described above.

2.8. In vitro cytotoxicity study

Cell cytotoxicity of the derivatives was carried out on JCRB0831 cell. The cells, grown in DMEM supplemented with 50% F12 medium, 10% FBS, 2 mM L-glutamine, penicillin G sodium, streptomycin sulfate and amphotericin B at 37 °C in a fully humidified, 5% CO_2, were seeded in a 96-well plate at a density of 8000 cells/well and incubated for 24 h. The serial dilutions of sample (in a range of 0.05–20 mg/mL) were added and incubated for another 24 h. The MTT in PBS (0.5 mg/mL) was then added and further incubated for 4 h. Formazan crystal was solubilized with 100 μL of DMSO. The absorbance was read with a microplate reader (SpectroMAX, USA) at a wavelength of 540 nm. Results were recorded as percentage absorbance relative to untreated control cells. The cytotoxicity results were used to calculate % relative cell viability as follows:

$$\%\text{Relative cell viability} = \frac{abs_{sample} - abs_{DMSO}}{abs_{control} - abs_{DMSO}} \times 100 \quad (2)$$

where abs_{sample} is the absorbance in a well containing sample, $abs_{control}$ is the absorbance for untreated control cells, and abs_{DMSO} is the absorbance of DMSO. IC_{50} values were extrapolated to 50% relative cell viability using linear regression analysis where the value can be obtained as the concentration of the polymers that is required to reduce the absorbance of cell viability to 50%.

2.9. Mucoadhesive study

2.9.1. Sub-micron mucin particle method

One % (w/v) mucin suspension (in 10 mM Tris base, pH 6.8) was applied with the ultrasonication (VCX750, Sonics & Materials, Inc.). One milliliter of 1% (w/v) mucin suspension was mixed with different concentrations of 0.05–0.5% (w/v) QCD23-*g*-CS or QCDCA22-*g*-CS under mild magnetic stirring. The particle sizes and zeta potential values were then measured by using photon correlation spectroscopy (NanoZS4700 nanoseries, Malvern Instruments) equipped with a 4 mW HeNe laser at a wavelength of 633 nm at 25 °C. The refractive index of both derivatives and water were set at 1.33. All experiments were performed in triplicate.

2.9.2. Surface plasmon resonance technique (SPR)

The mucoadhesive properties of QCD23-*g*-CS and QCDCA22-*g*-CS were determined according to the method modified from Takeuchi et al. (2005) and Thongborisute and Takeuchi (2008). Firstly, CMD500 (carboxymethyldextran hydrogel) sensor chip surface was covered by chitosan (molecular weight 22 kDa) with a mixture of 100 mM N-hydroxysuccinimide (NHS) and 400 mM 1-ethyl-3-(3-dimethylaminopropyl) carbodiimide hydrochloride (EDC). The remaining reactive esters were transformed into inactive amides by injection of 1 M ethanolamine HCl, pH 8.5. All immobilization were carried out at a flow rate of 50 μL/min. Mucin particle suspension at a concentration of 0.1% (w/v) was prepared in 10 mM acetate buffer (pH 4.5) as mentioned earlier (Petchsangsai

Table 1
Percentage of degree of N-substitution (DS), degree of quaternization (DQ) and EG encapsulation (%EE) of quaternized βCD grafted chitosan.

Quaternized βCD grafted chitosan	%DS[a]	%DQ[a]	%EE
QCD23-*g*-CS	23	66	59.3 ± 2.4
QCDCA22-*g*-CS	22	72	35.8 ± 2.1

[a] Determination by ^{1}H NMR method.

et al., 2010), which was injected over immobilized sensor chip surface at a flow rate of 30 μL/min. The 0.5% (w/v) of QCD23-*g*-CS and QCDCA22-*g*-CS was injected afterwards. The equilibrium baseline data were collected at each injection. The running buffer was 10 mM acetate buffer (pH 4.5). Polyacrylic acid (PAA, ~140 kDa) was used as positive control in this study. The parameter denoted as the refractive index unit (RIU) was then recorded on the home-built SPR imaging system equipped with a 7-channel flow cell, which was reported elsewhere (Petchsangsai et al., 2010). %RIU change was analyzed according to Eqs. (3) and (4) after the injections of samples and NaCl, respectively.

$$\%\text{RIU change} = \frac{\text{RIU baseline of sample RIU baseline of mucin}}{\text{RIU baseline of mucin RIU baseline of immobilized chitosan}} \times 100 \quad (3)$$

$$\%\text{RIU change (with NaCl)} = \frac{\text{RIU baseline of NaCl} - \text{RIU baseline of mucin}}{\text{RIU baseline of mucin RIU baseline of immobilized chitosan}} \times 100 \quad (4)$$

3. Results and discussion

3.1. Chemical structures of quaternized βCD grafted chitosan

The quaternized βCD grafted chitosan with different spacers were carried out by reacting the chitosan with O-*p*-toluenesulfonyl-β-cyclodextrin (Ts-CD) or β-cyclodextrin citrate (CDCA) under acidic condition at high temperature, leading to CD-*g*-CS or CDCA-*g*-CS, respectively (Chaleawlert-umpon et al., 2011; Gonil et al., 2011). In this study, the Ts-CD was prepared by using 10% (w/v) NaOH in order to increase a percent yield. The degree of tosylation was found to be 1.76, indicating that formation of ditosylation in the βCD backbone either the primary hydroxyl or secondary hydroxyl groups. The CD-*g*-CS was obtained through nucleophilic displacement of the tosyl group indicating the methylene space between chitosan backbone and βCD moiety. Therefore, one of two tosyl groups was displaced during grafting into the chitosan backbone, while the other still remained in the βCD moiety. In case of CDCA-*g*-CS, βCD citrate (CDCA) was used instead of Ts-CD. The CDCA was prepared by esterification of βCD with citric acid. The reactive cyclic anhydride intermediate of CA was generated via a dehydration of the adjacent carboxyl groups. Then it was reacted with the primary hydroxyl groups of βCD. The CDCA-*g*-CS was obtained through the amide formation between the amino groups of chitosan and the free carboxyl groups of CDCA. The degree of N-substitution (DS) of βCD moiety into the chitosan backbone, which determined by ^{1}H NMR, was 23% for methylene spacer (CD23-*g*-CS) and 22% for citric spacer (CDCA22-*g*-CS), respectively (Table 1). Quaternization of the CD23-*g*-CS or CDCA22-*g*-CS with GTMAC under acidic condition at high temperature, leading to water-soluble CD grafted chitosan. The chemical structures of QCD23-*g*-CS and QCDCA22-*g*-CS are shown in Fig. 1.

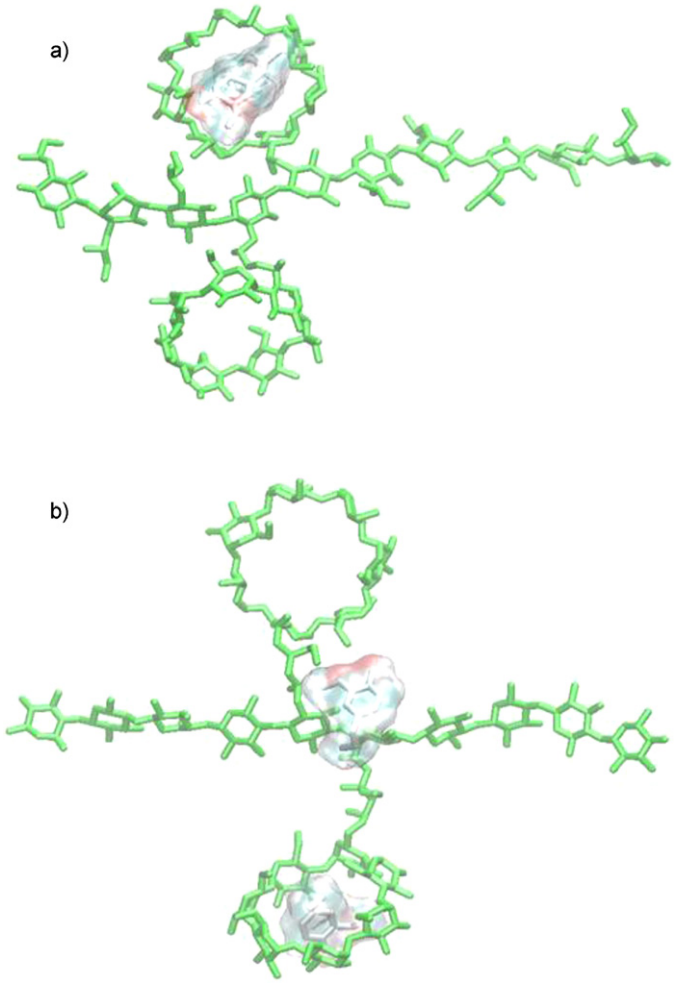

Fig. 2. Host–guest C—H:O interactions of 1:1 mole ratio inclusion complex between βCD-grafted chitosan (green sticks); QCD23-*g*-CS (a), QCDCA22-*g*-CS (b) and eugenol (gray spheres) in aqueous solution.

The physicochemical properties and chemical structure characterization were previously reported (Chaleawlert-umpon et al., 2011; Gonil et al., 2011). According to ^{1}H NMR, the degrees of quarternization (DQ) were calculated up to 66% QCD23-*g*-CS and 72% for QCDCA22-*g*-CS, respectively, defined as an introduction of quaternary ammonium moiety. Both derivatives exhibited excellent water solubility.

3.2. Computer modeling on inclusion complex formation between EG and quaternized βCD grafted chitosan

To understand binding interaction between EG and quaternized βCD grafted chitosan (QCD23-*g*-CS and QCDCA22-*g*-CS) at 1:1 mole ratio of inclusion complex, the same amount of βCD grafting was fixed at 20% in in silico modeling study. Models of EG and both quaternized βCD grafted chitosan in aqueous system subjected to molecular dynamic simulations are presented in Fig. 2. In most stable complex of QCD23-*g*-CS, hydrophobic moieties of EG molecules are enclosed within βCD. The hydrophilic portions of EG molecules are exposed to aqueous environment and associated with water molecules. Negative energy term results from EG binding interactions with βCD cavity of quaternized βCD grafted chitosan and their solubility as well as final complex (Table 2). During complexation, total free energy values of QCD23-*g*-CS (−8.79 kcal/mol) suggested that EG could be spontaneously encapsulated into βCD cavity at 25 °C, whereas the complexation of

Table 2
Comparison of the binding energy and thermodynamic characteristics of inclusion complex at 1:1 mole ratio of EG and quaternized βCD grafted chitosan in aqueous system.

Energy (kcal/mol)	QCD23-*g*-CS		QCDCA22-*g*-CS	
	Complexation	Absorption	Complexation	Absorption
Binding energy	−43.69	−33.57	−24.96	−39.51
Solvation energy	34.89	−49.46	34.27	−37.94
$\Delta G^{complex}$	−809.48	−859.49	−825.65	−794.03
$\Delta G^{derivatives}$	−792.99	−774.67	−839.99	−720.74
$\Delta G^{eugenol}$	−51.39	−35.35	−59.93	−35.35
Total free energy (ΔG)	−8.79	−83.04	9.31	−77.46

QCDCA22-*g*-CS would be energetically unfavorable due to the positive value (9.31 kcal/mol). Additionally, EG would be expected on a surface of both derivatives, which was presented as absorption energy. It was found that the EG absorption on a surface of QCD23-*g*-CS (−83.04 kcal/mol) would be more favorable than that of QCDCA22-*g*-CS (−77.46 kcal/mol). From these results, EG could be both enclosed in both βCD and absorbed on the surface of QCD23-*g*-CS, whereas EG preferred to be absorbed on chitosan backbone of QCDCA22-*g*-CS, but not inside βCD cavity.

3.3. EG encapsulation efficiency (%EE) of quaternized βCD grafted chitosan

%EE of EG in QCD23-*g*-CS and QCDCA22-*g*-CS was calculated at 1:1 mole ratio of EG and βCD in each derivative and were found at 59.3 ± 2.4% and 35.8 ± 2.1% for QCD23-*g*-CS and QCDCA22-*g*-CS, respectively (Table 1). Higher %EE of QCD23-*g*-CS could be attributed to more favorable total free energy both from inclusion complex and adsorption. Moreover, at 1% concentration of inclusion complex, it is possible that self-aggregation of quaternized βCD grafted chitosan could be formed by turning βCD as a hydrophobic core inside and quaternary ammonium moieties outside. According to AFM and TEM, a presence of these self-assemblies was found from only QCD23-*g*-CS with particle sizes determined in a range of 800–3000 nm (Sajomsang et al., 2011, 2012). It is possible that apart from inside βCD cavity, EG could allocate at hydrophobic core of these self-assemblies. However, this does not seem to be the case for QCDCA22-*g*-CS, where an absence of particle was observed under the microscopic observation (data not shown).

3.4. In vitro cytotoxicity of quaternized βCD grafted chitosan

The safety of QCD23-*g*-CS and QCDCA22-*g*-CS was evaluated over a range of concentrations (0.5–40 mg/mL) (Fig. 3). The numbers of lived cells significantly decreased about 50% at the first incubation (0.5 mg/mL). Moreover, only 10–20% of vital cells were found with an increase in polymer concentrations over 20 mg/mL. The results suggested that the cytotoxicity was likely to depend on the effect of positive charge from quaternary ammonium groups, which was previously reported by Sajomsang et al. (2011) and Peng et al. (2010). The concentration, which inhibited 50% cell growth (IC_{50}) values were determined and found at 1.2 mg/mL and 0.6 mg/mL for QCD23-*g*-CS and QCDCA22-*g*-CS, respectively. The result revealed that IC_{50} values of both derivatives are not significantly different.

3.5. In vitro release study

The %cumulative released profiles of inclusion complex are presented in Fig. 4. The freeze-dried powder was dissolved in simulated saliva buffer at pH 6.8. Inclusion complex of QCD23-*g*-CS and QCDCA22-*g*-CS showed fast release phase followed by delayed release profiles, which then reach the plateau level at 40% and 59%

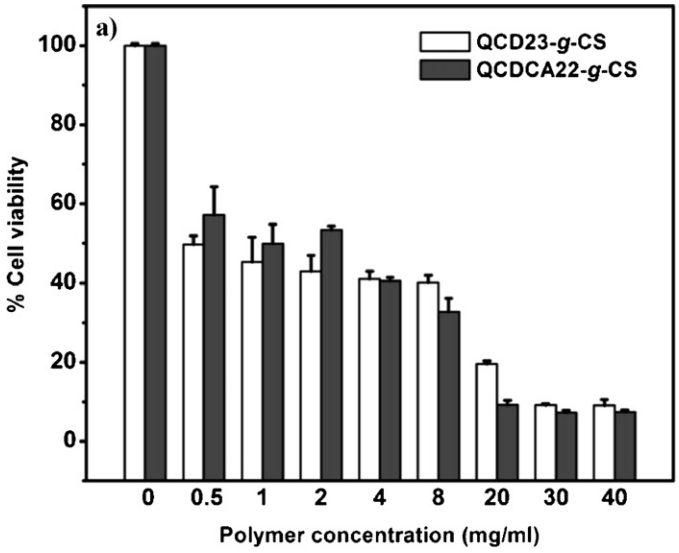

Fig. 3. Percentage of cell viability on mucosal cells after exposure with QCD23-*g*-CS and QCDCA22-*g*-CS at varying concentration from 0 to 40 mg/mL.

EG released, respectively. Nearly 100% of EG could release from βCD, which was used as a control in this study. A faster release phase could be due to the release of EG that was absorbed on the CS backbone of QCDCA22-*g*-CS. The EG release at a later phase is due to EG from the inclusion complex and the hydrophobic core of QCD23-*g*-CS assemblies. This possibly explained slower EG release from QCD23-*g*-CS as compared to the QCDCA22-*g*-CS. This result is in accordance with Prabaharan and Mano (2005) and Krauland and Alonso (2007). They proposed the chitosan containing βCD moiety as an alternative material for drug controlled release due to the presence of hydrophobic βCD cavity. Therefore, these derivatives are able to manage a sustained release of hydrophobic drug. Moreover, in our study it is possible that the EG could mostly adsorb on a linker of QCDCA22-*g*-CS, therefore the initial EG released from QCDCA22-*g*-CS inclusion complex was higher than QCD23-*g*-CS inclusion complex. Meanwhile, there would be many possibilities of EG encapsulation in QCD23-*g*-CS due to its structure. Some EG molecules might embed within βCD, whether include into a micelle core, or adsorb around a polymer surface. These factors need to be

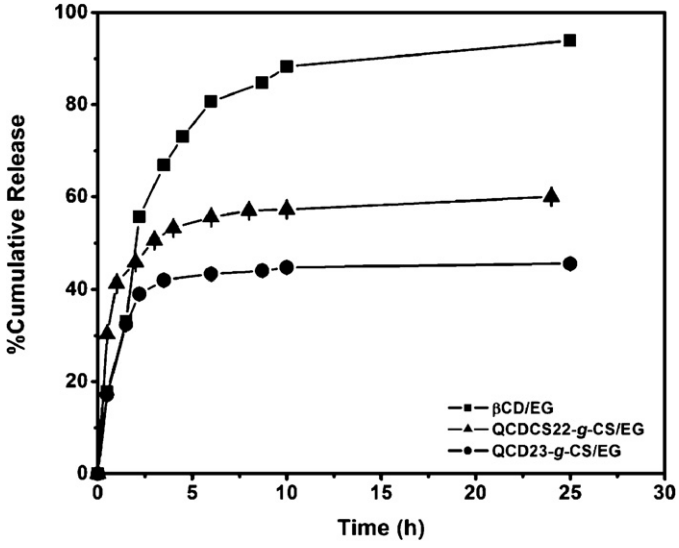

Fig. 4. Percentage of eugenol cumulative release from inclusion complex of βCD, QCD23-*g*-CS and QCDCA22-*g*-CS.

Table 3
Mucoadhesive characteristics of quaternized βCD grafted chitosan by SPR method.

Samples	%RIU change	
	Eq. (3)[a]	Eq. (4)[b]
Polyacrylic acid	27.65 ± 0.72	5.58 ± 1.40
Citrate-β cyclodextrin	−3.95 ± 0.22	−88.73 ± 0.46
Quaternized chitosan	75.57 ± 9.56	−8.74 ± 12.33
QCD23-*g*-CS	11.97 ± 3.21	−56.32 ± 0.41
QCD23-*g*-CS with eugenol	6.89 ± 0.35	−44.30 ± 1.40
QCDCA22-*g*-CS	87.51 ± 1.84	−2.18 ± 3.03
QCDCA22-*g*-CS with eugenol	80.79 ± 2.02	−3.69 ± 3.26

[a] After sample injection.
[b] After sodium chloride injection.

considered. However, the results suggest that inclusion complex of QCD23-*g*-CS and QCDCA22-*g*-CS with EG could control drug release.

3.6. Mucoadhesive study

3.6.1. Sub-micron mucin particle method

Mucoadhesive properties of water-soluble βCD grafted chitosan, QCD23-*g*-CS and QCDCA22-*g*-CS, with different spacers were investigated. According to our previous work, the QCD23-*g*-CS and QCDCA22-*g*-CS were firstly reported a mucoadhesive property (Chaleawlert-umpon et al., 2011; Sajomsang et al., 2011) based on the sub-micron mucin particle method. It was expected that the strong mucoadhesive property of the polymer would result in aggregation between polymer and mucin particles when the two species were mixed (Takeuchi et al., 2005). The change on both particle sizes and zeta potential values of the mucin particles were monitored (Fig. 5a and b). By increasing an amount of these derivatives, the zeta potential of the mucin particle slowly changed from negative to positive values. A rapid increase in mucin particle size was found in both QCD23-*g*-CS and QCDCA22-*g*-CS. There were no changes in case of native βCD (data not shown). Linear regression analysis was shown in Fig. 5c and Table 3. A correlation between polymer concentration and relative zeta potential (zeta potential at each polymer concentration (Z_C)/zeta potential of the starting mucin particles (Z_0)) was found where the slope values of QCD23-*g*-CS and QCDCA22-*g*-CS were found at −3.27, and −2.83 and respectively. It was revealed that a stronger affinity of QCD23-*g*-CS towards mucin was found than that of QCDCA22-*g*-CS. The critical concentrations ($Z_C/Z_0 = 0$) of mucin neutralization, were calculated as 0.28 and 0.33% (w/w) for QCD23-*g*-CS and QCDCA22-*g*-CS, respectively. It should be noted sub-micron particle method is mainly based on electrostatic interaction between quaternary ammonium group of mucoadhesive polymers and the negatively charged sialic acid and sulphonic acid residues of mucus or mucin particles, other forces such as hydrogen bonding (the hydroxyl and amino groups of chitosan may interact with mucus via hydrogen bonding) and hydrohobic forces bound to the mucin particles are therefore neglected (Takeuchi et al., 2005). In addition, the negatively charged effect of citrate linkage could not be observed through the sub-micron mucin test (Chaleawlert-umpon et al., 2011).

3.6.2. Surface plasmon resonance (SPR)

To understand mucoadhesion mechanisms of derivatives, SPR study was carried out, in which the mucoadhesive property of polymers can be counted in term of reflective index unit (RIU). The RIU response can increase or decrease depending on a sample passes over sensor chip surface (Petchsangsai et al., 2010). Both derivatives and their inclusion complex can anchor above mucin layers, and provide the equilibrium response of RIU. The percentages of RIU increment can be calculated by Eq. (3), and the results are shown in Table 3. It was found that %RIU responses

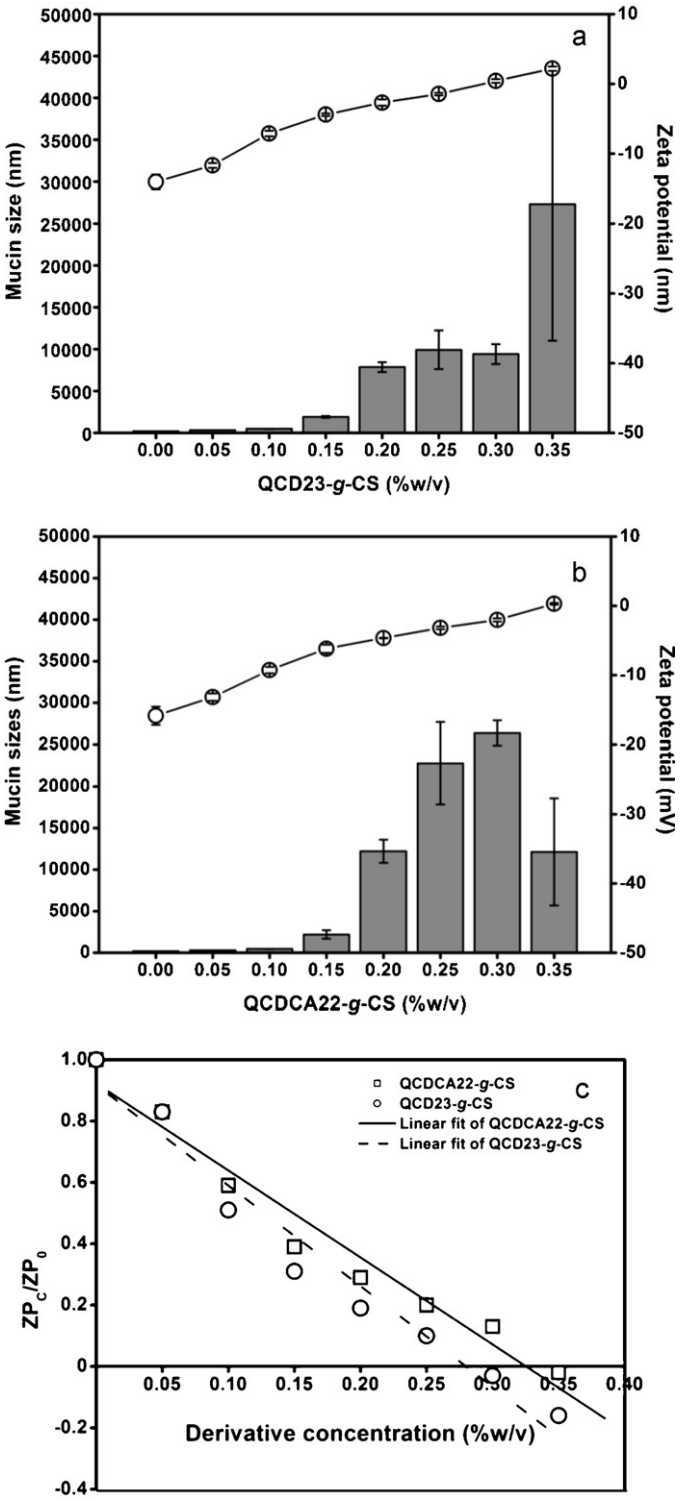

Fig. 5. Particle size (gray bar) and zeta potential (○) of sub-micron mucin solution at various concentrations of QCD23-*g*-CS (a) and QCDCA22-*g*-CS (b). Relative plot of relative zeta potential at each concentration and derivative concentration based on sub-micron mucin particle method (c).

were 11.97 ± 3.21 and 87.51 ± 1.84 for QCD23-*g*-CS and QCDCA22-*g*-CS, respectively while the %RIU change of PAA was only 27.65. Moreover, the highest %RIU change (75.57) was obtained from quaternized chitosan, which was another positive control in this study. It is important to note that %RIU responses were not significantly changed in case of inclusion complex with EG (6.98 ± 0.35

and 80.79 ± 2.02 of QCD23-*g*-CS and QCDCA22-*g*-CS, respectively). A higher in %RIU response means the more mucoadhesive efficiency. According to SPR result, the QCDCA22-*g*-CS showed mucoadhesive activity greater than the QCD23-*g*-CS.

In order to consider the mechanism of mucoadhesive binding between mucin and water-soluble βCD grafted chitosan, the strong ionic strength (3 M NaCl) was used since it is able to elute polymer attached on mucin layer. %RIU decreases can be estimated by Eq. (4). %RIU was found to be −56.31 ± 0.41 and −44.30 ± 1.40 of QCD23-*g*-CS and its inclusion complex, whereas the decrements of QCDCA22-*g*-CS and its inclusion complex are −2.18 ± 3.03 and −3.69 ± 3.26, respectively (Table 3). According to SPR and mucin particle method results, it is possible that the QCD23-*g*-CS and its inclusion complex could mainly attach to mucin via only electrostatic force while the QCDCA22-*g*-CS demonstrated different mechanisms. At the same concentration, the SPR results of the QCDCA22-*g*-CS were similar to that of polyacrylic acid, which was generally used as a mucoadhesive polymer (Takeuchi et al., 2005). The strong mucoadhesivity of QCDCA22-*g*-CS can be ascribed to hydrogen bonding of the carboxyl and hydroxyl groups from the citrate spacer. Hydrogen bonds between carboxylate anion of the citrate molecule could occur with mucus glycoprotein. Thus, both electrostatic attraction and hydrogen bonding were presumably attributed to stronger mucoadhesive response of the QCDCA22-*g*-CS. Nevertheless, CDCA itself did not show any mucoadhesive property (−3.95 ± 0.22 of %RIU change after sample injection and −88.73 ± 12.33 of %RIU decrease after NaCl injection). It should be noted that, the attachment between mucin and QCDCA22-*g*-CS could not be detected by using mucin-particle method, because the carboxylate anions at the citrate spacer could also repulse the negatively charged mucin particles (Chaleawlert-umpon et al., 2011).

4. Conclusion

Two types of water-soluble βCD grafted chitosan with different spacers were investigated. The EG encapsulation efficiencies of QCD23-*g*-CS were higher than that of QCDCA22-*g*-CS, which could be attributed to not only inclusion complex within βCD cavity, but also adsorption on chitosan chain as confirmed by computer modeling. The QCD23-*g*-CS showed slower release of EG than the QCDCA22-*g*-CS due to self-assembly formation of the QCD23-*g*-CS. Cytotoxicity was dependent on derivative concentration. The mucoadhesive property was investigated where mucoadhesivity of QCD23-*g*-CS occurred through electrostatic interaction while the QCDCA22-*g*-CS occurred through both hydrogen bonding and electrostatic interaction. This could be due to effect of spacers between βCD moiety and chitosan backbone. Although their inclusion complex with EG has been formed, these polymers could retain their mucoadhesive properties. The presence of spacer of water-soluble βCD grafted chitosan played an important role on inclusion complex, released profile and mucoadhesive property.

Acknowledgements

The authors wish to acknowledge the financial support from the Research, Development and Engineering (RD&E) fund through National Nanotechnology Center (NANOTEC), National Science and Technology Development Agency (NSTDA), Thailand (Project No. NN-B-22-EN7-94-51-20). Technical assistance from Dr. Boonsong Sutapun, Photonics Technology Laboratory, National Electronics and Computer Technology Center are appreciated.

References

Chaleawlert-umpon, S., Nuchuchua, O., Saesoo, S., Gonil, P., Ruktanonchai, R. U., Sajomsang, W., et al. (2011). Effect of citrate spacer on mucoadhesive properties of a novel water-soluble cationic β-cyclodextrin-conjugated chitosan. *Carbohydrate Polymers*, *84*, 186–194.

Fermeglia, M., Ferrone, M., Lodi, A., & Prici, S. (2003). Host–guest inclusion complexes between anticancer drugs and β-cyclodextrin: Computational studies. *Carbohydrate Polymers*, *53*, 15–44.

Gonil, P., Sajomsang, W., Ruktanonchai, U. R., Pimpha, N., Sramala, I., Nuchuchua, O., et al. (2011). Novel quaternized chitosan containing β-cyclodextrin moiety: Synthesis, characterization and antimicrobial activity. *Carbohydrate Polymers*, *83*, 905–913.

Illum, L., Farraj, N. F., & Davis, S. S. (1994). Chitosan as a novel nasal delivery system for peptide drugs. *Pharmaceutical Research*, *11*, 1186–1189.

Krauland, A. H., & Alonso, M. J. (2007). Chitosan/cyclodextrin nanoparticles as macromolecular drug delivery system. *International Journal of Pharmaceutics*, *340*, 134–142.

Muzzarelli, R. A. A. (1977). *Chitin*. Oxford, UK: Pergamon Press.

Muzzarelli, R. A. A. (2010). Chitins and chitosans as immunoadjuvants and non-allergenic drug carriers. *Marine Drugs*, *8*(2), 292–312.

Nuchuchua, O., Saesoo, S., Sramala, I., Puttipipatkhachorn, S., Soottitantawat, A., & Ruktanonchai, U. (2009). Physicochemical investigation and molecular modeling of cyclodextrin complexation mechanism with eugenol. *Food Research International*, *42*, 1178–1185.

Peng, Z. X., Wang, L., Du, L., Guo, S. R., Wang, X. Q., & Tang, T. T. (2010). Adjustment of the antibacterial activity and biocompatibility of hydroxypropyltrimethyl ammonium chloride chitosan by varying the degree of substitution of quaternary ammonium. *Carbohydrate Polymers*, *81*, 275–283.

Petchsangsai, M., Sajomsang, W., Gonil, P., Nuchuchua, O., Sutapun, B., Puttipipatkhachorn, S., et al. (2010). A water-solublemethylated N-(4-N,N-dimethylaminocinnamyl) chitosan chloride as novel mucoadhesive polymeric nanocomplex platform for sustained-release drug delivery. *Carbohydrate Polymers*, *83*, 1263–1273.

Prabaharan, M., & Gong, S. (2008). Novel thiolated carboxymethyl chitosan-g-b-cyclodextrin as mucoadhesive hydrophobic drug delivery carriers. *Carbohydrate Polymers*, *73*, 117–125.

Prabaharan, M., & Jayakumar, R. (2009). Chitosan-graft-b-cyclodextrin scaffolds with controlled drug release capability for tissue engineering application. *International Journal of Biological Macromolecules*, *44*, 320–325.

Prabaharan, M., & Mano, J. F. (2005). Hydroxypropyl chitosan bearing beta-cyclodextrin cavities: Synthesis and slow release of its inclusion complex with a model hydrophobic drug. *Macromolecular Bioscience*, *5*, 965–973.

Prabaharan, M., & Mano, J. F. (2006). Chitosan derivatives bearing cyclodextrin cavitiesas novel adsorbent matrices. *Carbohydrate Polymers*, *63*, 153–166.

Sajomsang, W., Ruktanonchai, U. R., Gonil, P., & Nuchuchua, O. (2009). Mucoadhesive property and biocompatibility of methylated N-aryl chitosan derivatives. *Carbohydrate Polymers*, *78*, 945–952.

Sajomsang, W., Gonil, P., Ruktanonchai, U. R., Pimpha, N., Sramala, I., Nuchuchua, O., et al. (2011). Self-aggregates formation and mucoadhesive property of water-soluble-cyclodextrin grafted with chitosan. *International Journal of Biological Macromolecules*, *48*, 589–595.

Ravi Kumar, M. N. V., Muzzarelli, R. A. A., Muzzarelli, C., Sashiwa, H., & Domb, A. J. (2004). Chitosan chemistry and pharmaceutical perspectives. *Chemical Reviews*, *104*, 6017–6084.

Sajomsang, W., Nuchuchua, O., Gonil, P., Saesoo, S., Sramala, I., Soottitantawat, A., et al. (2012). Water-soluble β-cyclodextrin grafted with chitosan and its inclusion complex as a mucoadhesive eugenol carrier. *Carbohydrate Polymers*, *89*, 623–631.

Shimpi, S., Chauhan, B., & Shimpi, P. (2005). Cyclodextrins: Application in different routes of drug administration. *Acta Pharmaceutica*, *55*, 139–156.

Song, L. X., Bai, L., Xu, X. M., He, J., & Pan, S. Z. (2009). Inclusion complexation, encapsulation interaction and inclusion number in cyclodextrin chemistry. *Coordination Chemistry Review*, *253*, 1276–1284.

Szejtli, J. (2004). Past, present, and future of cyclodextrin research. *Pure and Applied Chemistry*, *76*, 1825–1845.

Takeuchi, H., Thongborisute, J., Matsui, Y., Sugihara, H., Yamamoto, H., & Kawashima, Y. (2005). Novel mucoadhesion tests for polymers and polymer-coated particles to design optimal mucoadhesive drug delivery systems. *Advanced Drug Delivery Reviews*, *57*, 1583–1594.

Thongborisute, J., & Takeuchi, H. (2008). Evaluation of mucoadhesiveness of polymers by BIACORE method and mucin-particle method. *International Journal of Pharmaceutics*, *354*, 204–209.

Van De Manakker, F., Vermonden, T., Van Nostrum, C. F., & Hennink, W. E. (2009). Cyclodextrin-based polymeric materials: Synthesis, properties, and pharmaceutical/biomedical applications. *Biomacromolecules*, *10*, 3157–3175.

Zhan, H., Jiang, Z. T., Wang, Y., Li, R., & Dong, T. S. (2008). Molecular microcapsules and inclusion interactions of eugenol with β-cyclodextrin and its derivatives. *European Food Research and Technology*, *227*, 1507–1513.